339
8-5-66

COO-285

MASTER

AN EVALUATION OF THE ATOMICS INTERNATIONAL 1000 MWe FAST BREEDER REACTOR

PREPARED BY: REACTOR ENGINEERING DIVISION
CHICAGO OPERATIONS OFFICE
U. S. ATOMIC ENERGY COMMISSION

JULY 1966

DISCLAIMER

LEGAL NOTICE

Printed in USA. Price $3.00 . Available from the Clearinghouse for Federal Scientific and Technical Information, National Bureau of Standards, U. S. Department of Commerce, Springfield, Virginia 22151

COO-285
Reactor Technology
UC-80
TID-4500 (48th Edition)

AN EVALUATION

of the

ATOMICS INTERNATIONAL 1000 MWe

FAST BREEDER REACTOR

PREPARED BY: REACTOR ENGINEERING DIVISION
CHICAGO OPERATIONS OFFICE
U. S. ATOMIC ENERGY COMMISSION

JULY 1966

CONTRIBUTORS

Editing

AEC

C. Fies

Reactor Physics

ANL

H. Hummel
K. Phillips

AEC

C. Fies

LASL

M. Battat
G. Best
B. Carmichael
D. Dudziak
W. Hannum
R. La Bauve
G. Ragan
J. Vigil

Fuel and Materials

ANL

J. Ayer
R. Dunworth
J. Handwerk
C. Reinke

AEC

J. Purcell

Fuel Cycle Costs

AEC

A. Hosler

TABLE OF CONTENTS

LIST OF TABLES

LIST OF FIGURES

1.0 INTRODUCTION AND SUMMARY

1.1 Introduction

In January 1964, four 1000 MWe conceptual designs of a Liquid Metal Fast Breeder Reactor (LMFBR) were submitted to the AEC by Allis-Chalmers Manufacturing Company (A-C), Combustion Engineering (CE), General Electric Company (GE), and Westinghouse (W).[1] An evaluation of these four studies was performed for the AEC by Los Alamos Scientific Laboratory (LASL) and Argonne National Laboratory (ANL) with the results published in COO-279.[2] The conclusions drawn from these reports proved the feasibility of this type of reactor but no final decisions could be made regarding the selection of an ideal design.

In June 1965, Atomics International (AI) completed a conceptual design of a 1000 MWe LMFBR with the results published in NAA-SR-11378.[3] The AI ground rules were similar to those of the four previous studies, but the AI study did contain some notable differences; the sodium outlet temperature was decreased and private ownership of fuel was assumed. In addition, AI had access to the previous studies and was not operating under similar project schedule and financing arrangements.

This report is an evaluation of the AI design and is to supplement the results published in COO-279. The report discusses the similarities and differences between the AI design and the previous four designs. Also, the results of a review of certain nuclear properties of the AI study, as well as the results of a recalculation of some of the nuclear properties considered in COO-279 pertaining to the first four design studies, are given. A summary of the important results of this evaluation is given in Section 1.2.

The calculations and comments reported in this review are made to further the understanding of and assist in comparison of the nuclear and other parameters. No implication regarding the accuracy of any parameter is intended.

1.2 Summary

The evaluation is summarized by answers to the following questions:

(1) What are the similarities and differences between the present concept and the previous 1000 MWe studies?

The design is a modular configuration. The comparison with the previous design studies is illustrated by the following:

	A-C	CE	GE	W	AI
Geometry:	Annular	Cylindrical	Pancake	Modular	Modular
Fuel:	Oxide	Carbide	Oxide	Carbide	Oxide
Moderation:	Nil	Nil	BeO Uniform	C in Blanket	C in Blanket

The geometry does not strongly influence the materials selection. Geometrically, the AI concept is similar to the Westinghouse (W) design. Four distinguishing features between the AI and W designs are: (1) the degree of blanket moderation, (2) the degree of blanket power and module-to-module coupling, (3) the volume of the fast core in each module, and (4) the use of ten modules by AI and six modules by W.

A discussion of the quantitative significance of these features is given in Section 3.0.

(2) Does the concept have a potential for significant advantage over the other concepts?

Considering those aspects in which this concept differs from the previous four studies, some advantages are obtained. By using the small core volume of 327 liters per module with the high 25% fraction of fissile plutonium, the maximum void effect in the core region is kept below $1.00. The high blanket Doppler of -0.016 T dk/dT is useful in limiting the consequences of accidents involving a power rise in the blankets. The average enrichment of the inner radial blanket regions at equilibrium is 3.5% and the discharge enrichment is approximately 6%. This enrichment, combined with the graphite moderator, results in 40% of the total power coming from the blankets. The high blanket power allows the use of a smaller number of modules and a total core volume of 3,270 liters. The radial blankets achieve an average burnup of 49,000 MWD/MT. (The AI study gives fuel exposures in MWD/T where T is metric tons.) The fabrication and reprocessing contributions to fuel cycle costs are materially reduced as a result of this extended burnup.

(3) Has review of the study identified any new problem areas that were not previously identified?

The use of spectral coupling emphasizes the need for improved techniques for calculating space- and energy-dependent fluxes. The procedures and spectrum used to produce blanket cross sections become increasingly important as the blanket power fraction is increased.

The Doppler effect is concentrated in the blankets with a relatively small Doppler in the core due to its high enrichment. While this may be a tolerable situation due to the high blanket power fraction of 40%, it complicates the accident analysis. The postulated power split between the core and blanket as the accident progresses determines the Doppler feedback.

The review calculations indicate that a positive void coefficient exists in the radial blankets under certain conditions as discussed in Section 3.3. The void effect behaves differently in the radial blankets than in the core. The initial void in the blanket produces a negative reactivity change and becomes positive as the 100% void condition is approached.

(4) Does the study resolve, or contribute substantially to the resolution of, any outstanding problems?

The AI concept has a maximum void effect of less than $1.00 in the core while maintaining a breeding ratio of at least 1.2. The AI design supplements the W concept and provides further evidence that a compromise can be obtained between breeding ratio and void effect with the modular concept.

The stability of a coupled system has been considered in general terms by Avery.[4] Atomics International has extended and utilized the Avery approach to investigate the kinetic behavior of a modular concept. This application is a significant contribution to the understanding of the present and similar concepts.

(5) How did the evaluators' nuclear parameters compare with the AI values?

Argonne cross sections and codes were used to calculate the nuclear parameters of AI's design. With AI's geometry and composition, the k calculated by ANL was only 0.94. This was not surprising as the comparison calculations performed in Ref. 13 indicated that AI's estimates of critical mass were substantially below those of ANL. Reference 14 shows that the reason for this difference in k is due to the differences in Pu-239 and U-238 cross sections.

The method of increasing k to make the reactor critical was enlarging the core radius from 28.5 cm to 33.3 cm or, for other calculations, increasing the fissile content of plutonium from 23.2% to 26.8%. This change in the AI composition and geometry makes comparison of the calculated reactor parameters more difficult. However, any important differences would still be apparent.

Table 1.1 compares the important nuclear parameters. The evaluators' numbers take into account the variation in the parameters due to:

1. The method of increasing k to make the reactor critical with ANL's cross sections.

2. The effect of 2-D geometry using LASL's 2-D codes.

3. The effect of using different methods of calculating the ANL graphite cross sections.

The variation of the AI Doppler values contributes to the uncertainty of the positive Pu-239 contribution as explained in Section 3.4.

Table 1.1

Comparison of AI and Evaluators' Nuclear Parameters

NUCLEAR PARAMETER	AI	Evaluators
Sodium Void (100% Core Void) % $\frac{\Delta k}{k}$	$< -.25$	$-.49 \pm .12$
Doppler (Core) $T\frac{dk}{dt} \times 10^3$	$-1.84 \pm .46$	$-1.80 \pm .18$
Doppler (Core and Radial Blankets) $T \frac{dk}{dt} \times 10^3$	-16.6 ± 1.5	-14.3 ± 1.0
Breeding Ratio	1.30	$1.25 \pm .05$

(6) How do the economics of the five designs compare when evaluated on a consistent basis?

The fuel cycle costs of the five design studies were recalculated using a consistent set of ground rules including private ownership of fuel. The results are shown in Table 1.2. Further details on the assumptions and calculations are included in Appendix E.

Table 1.2

Recalculated Fuel Cycle Costs

	A-C	W	GE	CE	AI
Fabrication	.504	.458	.816	.626	.423
Reprocessing	.271	.240	.276	.264	.252
Pu Inventory	.603	.633	.427	.249	.426
Shipping	.052	.040	.054	.044	.036
Fabrication Charge	.081	.092	.090	.058	.060
Pu Credit	(.320)	(.549)	(.219)	(.387)	(.280)
Total	1.191	.914	1.444	.854	.917

(7) How have recent refinements to cross section data affected the results given in COO-279?

It is now believed that the ANL calculations used to modify the sodium void effect, as given in Table 3.3 of COO-279, were too negative. The Pu-239 fission cross sections used were too large at low energies as is further explained in Appendix D. Based on the latest Pu-239 data, ANL estimates the following values for complete voiding of sodium from the core:

Design Study	% Δk 100% Na Void	
	COO-279	Refined
AC	0.0	1.2
CE	1.0	2.9
GE	0.4	2.2
W	0.3	1.6
AI		-0.49

2.0 COMPARISON DATA

Figures 2.1 and 2.2 show the reactor core arrangements of the four previous studies and the AI study, respectively. Table 2.1 gives the characteristics of the five reference designs. A short narrative of the four previous designs is given in Section 2.0 of COO-279[2] and will not be repeated here.

The AI design employs ten small cores in an arrangement shown in Figure 2.2. Each core has a diameter of 1.87 feet with an active height of 4.2 feet. These cores are fueled with oxide fuel as are all blankets in the reactor. Each core is surrounded by annular rings of blanket and graphite. Further, the graphite ring is surrounded by more blanket material which is shared by adjacent modules. An 18-inch axial blanket is included in the design. The entire ten module assembly is surrounded by a ring of graphite followed by a final ring of blanket assemblies. Forty control rods are used in the reactor. Thirty rods are located in the graphite region to take advantage of the low energy flux and one rod is located in the center of each core.

THIS PAGE

WAS INTENTIONALLY

LEFT BLANK

Table 2.1

Characteristics of Reference Designs

		A-C	CE	GE	W	AI
I. General						
Breeding Ratio[1]		1.32	1.42	1.25	1.57	1.31
Doubling Time[2]	Yrs.	19.5	6.2	15.8	11.7	17.0
Sodium Void Worth (100% core voided)[1]	% Δk	+0.4	+2.4	+0.8	-0.15	-.25
Sodium Void Worth (100% core voided)[2]	% Δk	+1.2	+2.9	+2.2	+1.6	-.49
Maximum Reactivity (central Na void)[1]	$	-	-	4.2	.75	+.53
Doppler Coefficient[1]	$-T\frac{dk}{dt} \times 10^{+3}$	2.6	5	5	12	18.1
Fuel Cycle Costs[2] (private ownership)	mills/kw-hr	1.19	.85	1.44	.91	.92
Specific Power						
Core U+Pu Ceramic[1]	KW/kg	100	198	150	86	152
Core Fissile[2]	KW/kg	640	1680	920	520	634
Power Density Core[1]	KWt/liter	282	695	365	308	449
Core Power[1]	MWt	2125[3]	1868	2200	2170[3]	1388
Size						
Reactor Diameter	ft	16.0	10.0	14.2	13.6	15.0
Reactor Height	ft	6.0	5.5	5.0	8.3	7.2
Vessel Diameter	ft	20.0	16.5	18.0	18.0	26.0
Vessel Height	ft	25.0	40.7	33.0	36.0	41.5
Temperature						
Core Inlet	^{o}F	950	850	800	979	750
Clad Peak	^{o}F	1330	1400	1332	1400	1285
Fuel Peak	^{o}F	4615	2600	4700	2184	4800
Core Outlet	^{o}F	1200	1120	1100	1200	1075

Table 2.1 (Continued)

		A-C	CE	GE	W	AI
Fuel Bond		Helium	Sodium	Helium	Sodium	Helium
Coolant						
Sodium Flow	lb/Hr x 10^{-6}	114	113.6	95.4	128	87
Core Velocity	ft/sec	10	20	11.1	26.5	18.5
Loop Pressure Drop	psi	90	59.8	40	113	
Control						
No. of Units		48	12	85	21	40
Material		B_4C	B_4C	B_4C	B_4C	B_4C
Follower		UO_2	UC	Na	Voids + Na	Na

Table 2.1 (Continued)

			CORE & AXIAL BLANKET					RADIAL BLANKET				
			A-C	CE	GE	W	AI	A-C	CE	GE	W	AI
II.	Composition and Dimensions											
	Core Active Height	ft	4	2.5	2.0	6.3	4.2					
	Blanket Thickness	ft	.5	1.5	1.5	1.0	1.5	1.5	1.4	1.3	0.7	.40
	Core Fissile Metal Load	kg	3,690	1,155	2,304	3,686	2,187					
	Fast Core Load Metal	kg	17,760	8,913	12,828	23,420	8,010					
	Blanket Load Metal	kg	2,210	10,696	19,242	7,800	5,720	84,566	27,886	24,300[8]	56,886	63,760
	Core Load Ceramic	kg	20,200	9,400	14,600	25,200	9,080					
	Blanket Load Ceramic	kg	2,510	11,250	21,900	8,200	6,489	96,100	29,400	27,500[8]	59,800	72,332
	Core Volume	liters	7,520	2,895	6,030	7,050	3,260[13]					
	Fuel Fraction[5]	%	29.4	25.6	34.8[6]	29.4[7]	31.0	55	45	50.7[8]	55	49.1
	Sodium Fraction	%	40	66.5	46.4	55.1	53.8	30	43	32.1[8]	25	38.1
	Steel Fraction	%	30.6	7.9	18.8	15.5	15.2	15	12	17.2[8]	20	12.8
III.	Pins											
	Fuel Pin Clad O.D.	in.	0.30	0.30	0.25	0.30	0.25	0.607	0.45	0.50	0.464	0.34
	Clad Thickness	in.	0.028	0.011	0.015	0.010	0.015	0.015	0.016	0.020	0.020	0.010
	Sodium Bond Gap	in.		0.010		0.006			0.011			
	Pellet O.D.	in.	0.24	0.259	0.22	0.268	0.214	0.574	0.396	0.45	0.420	0.320
	Pellet I.D.	in.	0.10		~ 0.06[4]							
	Compartment Length	in.	3	102	96	12						
	Active Core Height	in.	48	30	24	75	50					
	Active Blanket Height	in.	6	36	36	24	18	72	54	36 & 60	87	50
	Gas Reservoir	in.	6	15	36	Vented	21		8	18	13	
	Over-all Pin Length	in.	72	102	96	102	113	72	63	64	102	

Table 2.1 (Continued)

			CORE & AXIAL BLANKET					RADIAL BLANKET				
			A-C	CE	GE	W	AI	A-C	CE	GE	W	AI
IV.	Assemblies											
	Assembly Across Flats	in.	4.45	6.241	8.75[8]	5.104	4.875					
	Triang. Pitch of Pins	in.	0.375	0.468	0.338	0.426	0.356	0.69	0.539	0.565	0.496	0.418
	Pins per Assembly	no.	123	169	470	120	168	37	127	208	91	126
	Assemblies in Region	no.	498	157	225	252	180	858	156	108	357	504
	Total Pins in Region	no.	61,254	26,533	105,750	30,240	30,240	31,709	19,812	22,464	32,487	63,504
	Core Enrichment Av.	%	20.8	13.0[9]	18.0[9]	15.7	25.0	0.3	0.3	0.3	0.3	3.5
	Pellet Fabrication		Extruded	Cast	Pressed	Pressed	Pressed	*	*	*	Pressed	*
	Material		Oxide	Carbide	Oxide	Carbide	Oxide	*	*	*	Oxide	*
	Density	%	95	99	86	90	86	*	*	*	90	*
	Density	gm/cc	10.4	13.6	9.6	12.3	9.52	*	*	*	9.7	*
	Conductivity	BTU/hr-ft-^{o}F	1.6	10.5	1.6	11	1.88	*	*	*	1.6	*
	Stoichiometry			Hyper		Hypo						
V.	Power and Flux											
	Power, Av.	MWt	2,125	2,143[11]	2,408[8]	2,170	1,513	375	358	92[8]	330	937
	Lineal Power, Av.	KW/ft	8.6	28.2	10.4	12.0	11.1	2.0	3.1	1.1[8]	2.4	5.5
	Lineal Power, Max.	KW/ft	13.1	43.7	22.7	29.1	22.7					18.8
	Peak to Av. Power		1.52	1.55	2.18	2.42	2.04					3.33
	Median Fission Energy[1]	kev	190	302-311	110-139		210					73.0
	Av. Neutron Lifetime[1]	x 10^{7} sec	3.7	4.2	5.7	3	3.2					
	Effective Delayed Neutron Fraction[1]		.0032	.0040	.0033	.004	.00335					
	Core Pin Length	ft	245,000	66,400	211,500	189,000	127,008					
	Blanket Pin Length	ft	30,600	95,000	317,250	60,480	232,848	190,000	104,500	67,000	145,000	198,979

*Same as core

Table 2.1 (Continued)

			CORE & AXIAL BLANKET					RADIAL BLANKET				
			A-C	CE	GE	W	AI	A-C	CE	GE	W	AI
VI	Stress											
	Clad Stainless Steel		316	19-9DL	316	316L	304					
	Gas Release	%	75	11	70	30	100					
	Stress Thermal, Max.	psi	22,400[10]	22,000	21,000	18,000[10]	16,900					
	Stress Pressure, Max.	psi	12,000	6,000	8,600	Vented	Vented					
	Yield Stress (Room Temp.)	psi	30,000	33,000	30,000		30,000					
	1000 hr. creep rupture[12]	psi	12,000	13,000	9,000		15,800					
	Fuel Pressure Drop	psi	6.5	16.1	25	35.9						
	Heat Flux Av. BTU/hr-ft^2 x 10^{-6}		.373,	1.22	1.0	0.52	0.60					
	Heat Flux Max. BTU/hr-ft^{2}x 10^{-6}		.57	1.87	1.14	1.26	0.83					
	Gap Factors BTU/hr-ft^2 - ^{o}F		1,000		<4,000		1,500					
VII	Cost[1]											
	Fabrication	$/kg	350	124	143	200	261[14]	50	78	75	60	69
	Fabrication	$/assembly	12,300	15,500	20,400	24,800	17,160	5,060	14,000	14,200	9,550	
	Fabrication	$/core x 10^{-6}	6.14	2.43	4.60	6.24	3.09	4.34	2.18	2.22	3.41	
	Fabrication	$/pin	100	91.6	43.7	206	78	136.9	110.0	98.8	172.1	
	Fabrication	$/pin-ft	16.6	10.8	4.55	24.2	8.6	22.8	20.0	18.8	23.6	

[1] Per contractor calculations
[2] Per evaluator calculations
[3] Includes axial blanket
[4] Operating
[5] Includes void
[6] Includes BeO
[7] Includes cermet
[8] Data from errata to final report
[9] Zoned
[10] Estimated
[11] Includes control assemblies
[12] At 1400^{o}F
[13] Includes control rod region
[14] Fast Region

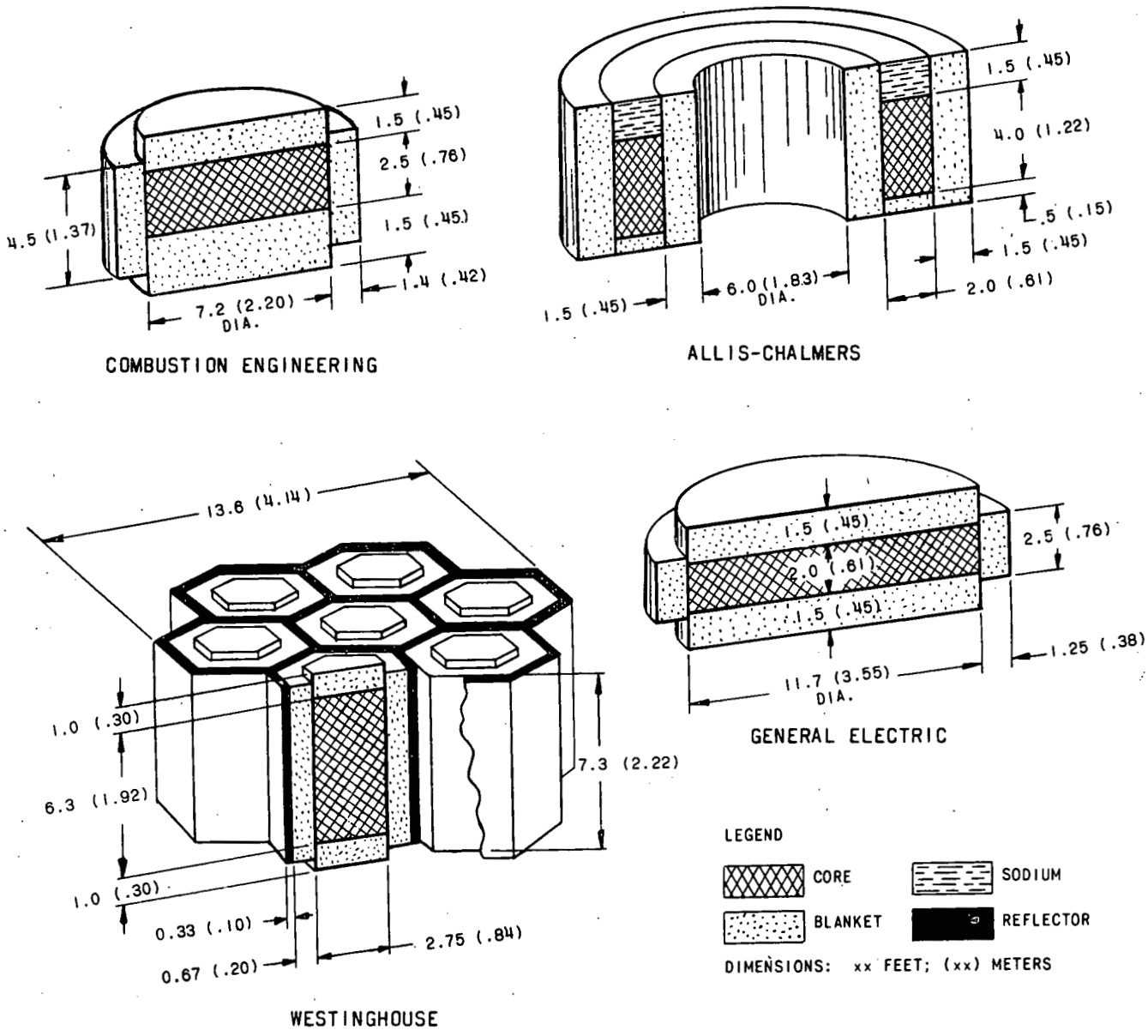

Figure 2.1

REACTOR CORE ARRANGEMENTS
FOUR 1000 MWe DESIGN STUDIES

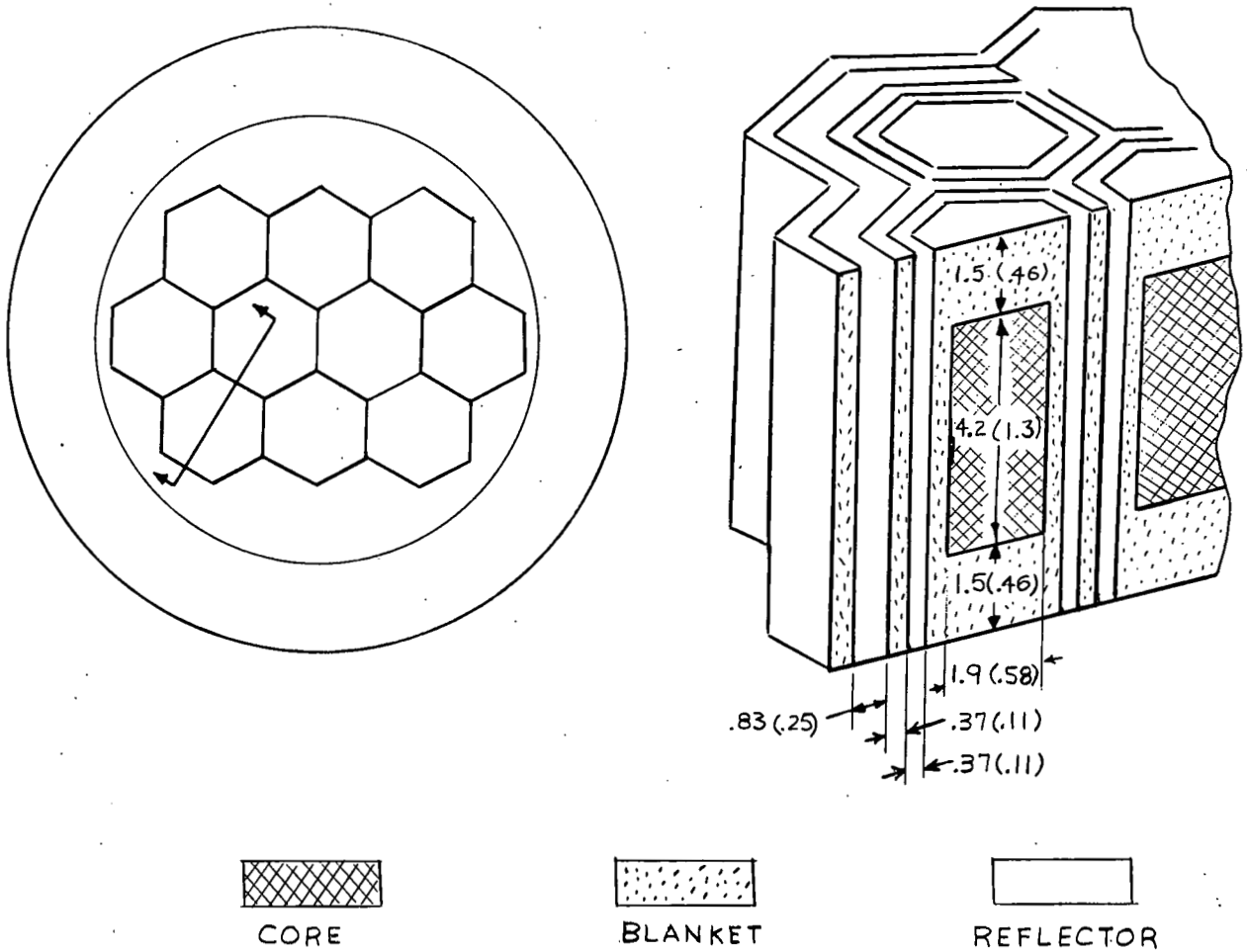

Figure 2.2 AI Reactor Core Arrangement

3.0 NUCLEAR CHARACTERISTICS

3.1 Introduction

Certain nuclear properties of the AI 1000 MWe Feasibility Study have been reviewed. The intent of this review is two-fold:

1. To compare the AI nuclear design with the previous four designs.

2. To determine how the nuclear parameters of AI's design, using AI's calculational methods, compare with independent methods of calculation.

Two independent methods of calculation were used. Los Alamos Scientific Laboratory (LASL) used AI's cross sections as input to their codes. Both 1-D and 2-D calculations were performed using diffusion theory and transport theory. The model LASL used for their calculations is explained further in Appendix B.

Argonne National Laboratory (ANL) used a completely independent method of arriving at cross sections using only AI geometry and composition as input. One-D diffusion calculations were performed using ANL cross sections and codes. The ANL method calculated a k of .935 to .948 depending on the graphite cross sections used. The reason for this discrepancy in calculated k is that the Pu^{239} fission cross sections used by ANL were lower than those used by AI in the important energy range, while the capture cross sections of U^{238} and Pu^{240} were higher. The cross sections were compared in Ref. 14. The reactor was made critical by varying the core radius and by enriching the core region. The ANL calculational method is discussed further in Appendix C.

3.2 Comparison of Nuclear Parameters

The intent of the design study was to obtain a concept with significantly improved safety characteristics over those realized in other ceramic-fueled Pu-U concepts, without undue penalty in fuel cycle costs. The measure of merit proposed (AI, Page III-A-1) included Doppler coefficient, sodium void reactivity effects, breeding ratio, prompt neutron lifetime, core fissile loading, regional peak-to-average power ratios, fast-to-blanket region power, and delayed neutron fraction.

The values reported for each of these measures of merit are given in Table 3.1. Also included are the corresponding values, where available, reported in each of the previous 1000 MWe studies.

The data reported show some significant improvements in Doppler, Na void, and prompt neutron lifetime has been achieved at little sacrifice in breeding ratio and fuel cycle costs. Of these, the prompt neutron lifetime is dismissed by AI as being of small consequence (AI, Pages III-A-1, III-A-2, and III-A-3); therefore, no attempt has been made to confirm the reported difference. The following parts of this section comment on the remaining parameters, either in terms of the values calculated, the procedures used, or the significance of the results obtained.

THIS PAGE

WAS INTENTIONALLY

LEFT BLANK

Table 3.1

Comparison of AI Selected Measures of Merit
As Reported in Design Studies

	AI	A-C	CE	GE	W
Isothermal Doppler Coef. ($T \frac{dk}{dT} \times 10^3$)					
Entire module	-18	-2.6	-5	-5	-12
Core region	-2.3				
Na Void Effect (%Δk)					
Core	-0.25	+0.4	+2.4	+0.8	-0.1
Worst case	+0.53			+4.2	+0.75
Breeding Ratio	1.30	1.32	1.42	1.25	1.57
Prompt Neutron Lifetime (μsec)	2.1	0.37	0.42	0.57	0.3
Fissile Loading (kg)	2718(a) 3053(b)	3696	1187	2362	3709
Peak-to-Average Power					
Core	1.45	1.52	1.55	2.18	2.42
Blanket	2.36				
Equilibrium Blanket Power Fraction	0.4	0.15	0.25	0.12	0.13
Delayed Neutron Fraction	0.00335	0.0032	0.0040	0.0033	0.0040

(a) AI, Table III-B-1
(b) AI, Table II-B-1 (Initial loadings)

3.3 Sodium Void Effect

General

As can be seen from Table 3.1, there is an apparent advantage to the AI proposal with regard to the sodium void effect. The reason for this seems clear. The core region is comparatively small; only 327 liters per module and the fissile percentage of plutonium of this region in the equilibrium condition is 25%.* The high fissile fraction causes the spectral component of the sodium void to remain small (though positive). The small volume plus an L/D of 2.25 cause the core islands to have a relatively large negative leakage component. The result is a situation where voiding of the core region of the reactor is negative except for the maximum positive condition of a central void where an effect of +53¢ is obtained.

Complete Void of the Core Region

The results of the review calculations are given in Table 3.2. The case of complete removal of sodium from the core region can be summarized as follows:

		$\%\Delta k$
(1)	AI	-0.25 to -0.42
(2)	LASL (2-D)	-0.36 to -0.60
(3)	ANL	-0.38 to -0.62

The range of values can be explained by: (1) AI calculated different values depending on the cross section methods used, their final result (Table II-B-1) states the void as $<$ -\$0.75 (-0.25 Δk); (2) LASL results varied when transport and diffusion theory was used, transport theory gave the less negative value of -0.36% Δk and (3) with ANL cross sections the reactor was substantially subcritical (see Section 3.1), the range of void effects depends on how the reactor was brought critical since the void effect is a function of enrichment and core volume.

Based on the review calculations, the core void effect calculated by AI may be slightly pessimistic. The evaluators' range of values for 100% void of the fast region could be given as $-.49 \pm .12\% \frac{\Delta k}{k}$ whereas the AI value is stated as $< -.25\% \frac{\Delta k}{k}$.

---

* The fissile Pu percentage is given as 25% in Table II-B-1 as well as other sections of the AI report. The atom densities (AI, Table III-B-2) give a fissile Pu percentage of 23.2%. The latter value was used in the physics calculations.

Blanket Only Voiding

The situation shown in AI Figure III-B-1 indicates that a positive void situation might exist in the radial blankets. The void worth starts going positive with increasing radius, especially in the outer radial blanket.

Argonne performed volume-wise sodium voiding calculations in the radial blankets. Removal of half the sodium in the blankets gave -0.176% Δk. When all sodium was removed, the void effect was +0.143% Δk. The ANL results also showed that there was little change in the total void effect when going from 50% to 100% void in the core plus radial blankets.

The net results are postulated in Figure 3.1. As the fraction of voids is increased, the fast region reactivity becomes more negative while the radial blanket regions have a minimum and make a positive contribution at high void fractions.

Table 3.2

Sodium Void Effect for the AI 1000 MWe Design

	% Δ k		
	100% Void Fast Region	50% Void Fast Region	50% Void Fast and Blanket
AI	-.25[a] -.42[b]		
ANL (Large Radius)[c]	-.380[e]	-.158[d] -.143[e] -.123[f]	-.273[d] -.288[e] -.283[f]
ANL (Enriched)[g]	-.624[e]	-.258[d] -.235[e] -.208[f]	-.405[d] -.415[e] -.400[f]
LASL (2-D)	-.60[h] -.36[i]		
LASL (1-D)	-.24[j] +.04[k]		

Other ANL results

50% Na void Blk. only [g] -.176

100% Na void Blk. only [g] +.143

100% Na void Fast and Blk. [g] -.423

a. AI Table II-B-1 p. II-B-2.

b. AI Table III-B-7 p. III-B-12

c. Core radius expanded from 28.5 cm to 33.3 cm to make k = 1.

d. ELMOE averaged σ_{er} for carbon.

e. Average of ELMOE and 1/E σ_{er} for carbon.

f. 1/E σ_{er} for carbon.

g. Core enrichment increased from 23.2% to 26.8% to make k = 1.

h. 2-D CRAM diffusion theory.

i. 2-D DDK transport theory.

j. 1-D CRAM diffusion theory.

k. 1-D DTF - This calculation seems to be overly sensitive to the reflector savings used. With a constant 20 cm reflector savings, rather than 25 cm with Na voided, the Na void is -0.69% Δk.

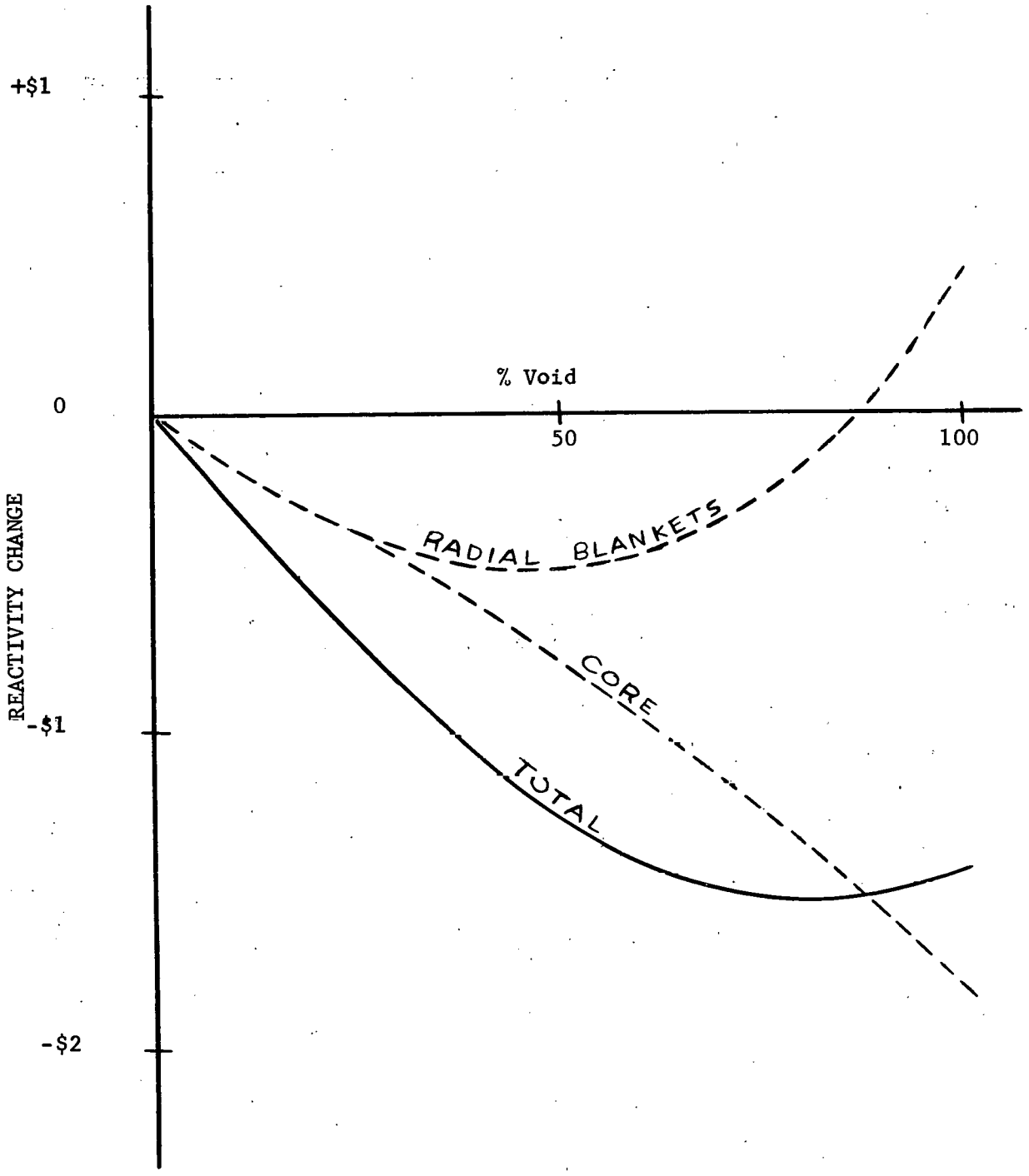

Figure 3.1 Reactivity Change vs. % Void
AI 1000 MWe Design

3.4 Doppler Effect

Table 3.3 shows the results of the Doppler calculations. These results may be summarized as follows:

(1) AI quotes a Doppler coefficient in the core of -1.84 ± .46* while ANL calculates a value of -1.80 ± .18.

(2) AI quotes a Doppler coefficient in the core plus blanket of -16.6 ± 1.5 while ANL calculates -14.3 ± 1.0.

The uncertainty of the numbers may be explained as follows:

(1) Throughout the report, AI neglected the positive fissile Pu contribution to the Doppler coefficient. ANL verifies that this may in fact be correct but the uncertainty in the AI numbers above take this Pu effect into account.

(2) The ANL values vary with the method of increasing k to make the reactor critical.

There are some other aspects of the Doppler effect that are worthy of comment. The report suggests a relative weighting of the fast region to blanket region Doppler effect of 3 to 1 (AI, Page III-C-44). This is obtained from consideration of the relative heating rates and coolant flow rates between fast and blanket regions to yield an effective Doppler coefficient of -8.0. Elsewhere in the report (Page III-B-1, Page II-B-2) the Doppler coefficient is given as -18.1; the sum of the core and blanket. The question of relative weighting would have to be studied in each postulated accident as it would depend strongly on the relative heating rates. There would also be the added complication of the Doppler being a strong function of burnup due to the change in blanket power.

In an accident that involves a temperature excursion rather than a power excursion (e.g., loss of flow), two effects may limit the effectiveness of the Doppler coefficient. In a temperature excursion in the fast region only, the Doppler effect for the fast region alone is effective, and for a temperature excursion in a single module, the reactivity sharing factor (0.13-AI, Page III-B-5) must be applied for all reactivity compensations, including the Doppler effect unless the module becomes critical independently.

* All Doppler coefficient numbers have units of $T \frac{dk}{dt} \times 10^{-3}$

Table 3.3

Doppler Coefficient for the AI 1000 MWe Design

	$T\frac{dk}{dT} \times 10^3$	
	Fast Region Doppler	Fast and Blanket Region Doppler
AI[a]	-2.30	-18.1
AI (Table III-B-5)[b]	-1.38	-15.1
ANL (Large Radius)[c]	-2.00[d]	-12.9[d]
	-2.00[e]	-13.8[e]
	-2.00[f]	-14.4[f]
ANL (Enriched)[c]	-1.57[d]	-14.0[d]
	-1.62[e]	-14.8[e]
	-1.64[f]	-15.4[f]

a) AI, Table II-B-1, p. II-B-2

b) AI, Table III-B-5, p. III-B-10 where the positive contribution of Pu-239 is taken into account.

c) See footnotes c and g, Table 3.2

d) ELMOE averaged σ_{er} for carbon

e) Average of 1/E and ELMOE σ_{er} for carbon

f) 1/E averaged σ_{er} for carbon

3.5 Breeding Ratio

Atomics International reported a breeding ratio of 1.30. This consisted of a core and radial blanket contribution of 1.07 and an axial blanket contribution of 0.23. These numbers were calculated by static physics calculations at the mid-point of the equilibrium fuel cycle using the atom densities from AI Table III-B-2.

Los Alamos has used the data from AI Table IV-B-3 to determine an implied breeding ratio of 1.31 as explained in Appendix A. The data in AI Table IV-B-3 was used in the AI economic analysis and was based on burnup calculations.

Table 3.4 summarizes the results of the review calculations. The radial breeding ratio calculated by ANL using an independent set of cross sections showed good agreement with the AI value. The radial breeding ratio (core plus radial blankets using a 1-D code) gave a value of 1.06 in agreement with the AI value of 1.07.

Los Alamos performed a 2-D 15-group calculation as explained in Appendix B with the breeding ratio results summarized in Table 3.5. This calculation took the axial blankets into account with a resulting breeding ratio of 1.25.

The value of the breeding ratio depends on some uncertain factors especially with this complicated modular geometry. The reflected boundry condition ($d\emptyset/dr = 0$) estimates the actual situation where the outer modules of the reactor are bounded on the inside by identical modules and on the outside by graphite. Any leakage over the amount calculated by the reflected boundry condition ($d\emptyset/dr = 0$) will detract from the breeding ratio. Los Alamos has calculated the effect of a free boundry and the radial breeding ratio decreased from 1.08 to 0.72. Any additional leakage, however, would be made up, at least in part, by breeding in the peripheral blankets.

Based on the evaluators results above, the breeding ratio of the AI 1000 MWe design could be stated as $1.25 \pm .05$.

If the breeding ratio is assumed to be 1.2, and if the quoted thermal performance is achievable, the doubling time as defined in Ref. 2, Table 3.6 would be approximately 17 years. This is comparable with what was obtained for the previous oxide design studies.

Table 3.4

Breeding Parameters for the AI 1000 MWe Design

	Total Breeding Ratio	Radial Breeding Ratio[a]	Core Conversion Ratio
AI (Page III-B-6)	1.30	1.07	-
AI (Economics)[b]	1.31	-	.416
LASL (2-D)	1.24	1.01	-
LASL (1-D)	-	1.08	-
ANL (Large Radius)	-	1.06	.444
ANL (Enriched)	-	1.06	.376
LASL (Free Outer Boundry)	-	.72	-
LASL (Reflected module, blanket replacing graphite moderator)	-	1.30	-

[a]The breeding ratio calculated by a 1-D code. The axial blanket contribution is not included.

[b]See Appendix A.

Table 3.5

Contributions to AI Net Breeding Gain[a]

	From Report (III-B-6)	Inferred from AI Economics[b] (IV-5)	LASL 2-D Reflected Module[c]
In Fast Region	1.07-0.95[d] =0.12	-0.37	-0.29
Inner Radial Blanket		0.24	0.22
Outer Radial Blanket		0.11	0.15
Axial Blanket Over Fast Region	0.23-0.05 =0.18	0.11	0.03
Axial Blanket Over Inner Blanket		0.08	0.07
Axial Blanket Over Outer Blanket		0.03	0.07
Exterior and Peripheral Blanket		0.11	
Total	0.30	0.31	0.25

[a] These figures reflect the net change in fissile content in each region, relative to the total fissile loss. Only the total is simply related to a breeding ratio.

[b] See Appendix A.

[c] See Appendix B for description of procedures and approximations used in review calculations. These figures are based on AI supplied cross sections and compositions. Thus, they evaluate only the effect of using 2-D S_n cell calculations rather than the AI synthesis method.

[d] These figures represent the power split (AI, Table II-B-1).

3.6 Other Nuclear Parameters

Fuel Loading

The reported loading of 2800 kg compares favorably with the other high leakage concepts (3700 kg). The former figure, however, should be corrected for finite geometry. The LASL review calculations (Appendix B) indicate that the reactivity allowance for axial leakage is quite reasonable. The radial leakage into the peripheral blanket, however, must be considered as lost, insofar as reactivity is considered. Thus, some weighting of reflected cell and of a single cell can be used to estimate the 10-module reactivity. While no quantitative estimate has been made, a 10% loading penalty might be reasonable. If the ANL cross sections are used, the volume of the core of each module would have to be increased by 35% to obtain criticality. The same result could be obtained by increasing the fissile percentage of Pu from 23.2% to 26.8%.

Peak to Average Power

The AI radial power shape factors were taken directly from their radial 1-D fission distributions (AI, Page III-B-6). A peaking factor of 1.25 was factored into the blanket power shape to account for the variation in enrichment from 0 to 7% (AI, Table III-B-19). The axial power shape factor of 1.25 was obtained from an axial 1-D diffusion calculation through the fast region of the module. It is not clear that an allowance has been made for power shifts during the cycle.

The peak to average powers for a reflected module are compared below:

Region	AI Report	2-D S_4	1-D ANL
Fast	1.45	1.41	1.42
Radial blankets, excluding axial regions	1.89[a]	1.78	1.79
All axial blankets	--	2.90	--
Radial blankets, including associated axial regions	2.36[a]	2.83	--

[a] Includes peaking factor of 1.25 due to variation of fissile Pu from 0 to 7%.

Control

The AI, Table III-B-8 suggests 7% Δk total control swing is needed for the AI core; 7.7% Δk was calculated as the control worth provided by the reference configuration. The 0.13 sharing factor (AI, Page III-B-14) implies a single, central module has $\simeq$ 0.91% Δk control. Half of this (0.45% Δk or $\simeq$ \$1.3) is associated with the central control rod, so that the AI single rod criterion of Page II-B-12 is not met. The AI Table III-B-1 lists a maximum control rod worth of \$1.27. The comparison of control

worth with that available from Doppler (AI, Page II-B-12) and the functional control assignments (AI, Page III-D-12) are based on a presumed adjustment of control worths, so as to equalize the worth of fast region and blanket region rods (AI, Page III-B-14) and obtain a maximum single rod worth of $\simeq$\$1.

Consideration of the effect on control rod worth of sodium voiding may preclude the indicated use of rare earth control material in that this material would be particularly sensitive to the reduction in worth as a result of spectral hardening. Along the line of alternate control materials, the comparison of Ta and B_4C on AI, Page III-D-17, is confusing. From the figures given in AI, Table III-D-1, the use of Ta as a control material appears attractive relative to full enriched $B_4{}^{10}C$.

Power Fraction and Median Neutron Energy

The power fraction and median neutron energies are compared below. It is seen that the 1-D diffusion theory representation is generally adequate for a single cell. The ANL values are different due to increase in fissile Pu from 23.2% to 26.8% in the core.

Factor	AI Report	LASL 2-D S_4	ANL 1-D
Power Fraction			
Fast Region	0.57	0.58	0.62
Radial Blanket	0.38	0.38	0.33
Axial Blanket	0.05	0.04	0.05
Median Energy of Neutrons producing Fission (Mev)			
Fast Region	0.21	0.25	0.27
Blankets	0.07	0.003	--

Other Comments

There are a number of relatively minor factors in the report that detract from what is otherwise a thorough report.

A distinct confusion in terminology is apparent. In the AI report, "Core" is used to refer to the fast region and to the fast and blanket regions combined (AI, Page III-B-1). "Thermal" is inappropriate as a description of the blanket. "Coupled" is used to refer to the coupling between modules and the coupling between fast and blanket regions. The change from "MOFT" (AI, Sections I and II) to "SCCR" (AI, Section III) presumably is without technical significance. The significance of the term "flux-trap" is not indicated. In this review, the fast, driving (high enrichment) region is referred to as the "fast region"; the blanket, including the graphite region, as "blanket." "Core" is used to denote the fast region and the central control regions. "Coupling," in this review, is taken as relating to module-to-module coupling only.

Some confusion also exists in certain design details. For example, the control rod design reflected in the nuclear design calculations (AI, Table III-B-2) differs from that used for control rod heating calculations (cf., AI, Drawing 14, Fig. III-B-15). Table II-B-1 lists rare earth blanket control; calculations (AI, Page III-B-18) are for B_4C. The basis for the atom densities for the control channel (AI, Table III-B-2) is obscure.

A somewhat more explicit differentiation in the report between the reference concept and various models used for surveys would have been helpful.

The plutonium production information given in Table III-B-15 is said to have been used to calculate the fuel cycle costs in Section IV, Economics. The total gain in fissile plutonium given in the table does not allow a total depletion credit as large as that given in Section IV. The table values include material that would be lost during fabrication and reprocessing (which is how the second footnote of Table III-B-15 should read) and therefore, if losses are considered, the discrepancy between Table III-B-15 and Section IV is greater.

Concerning Section IV; (1) the axial blanket fabrication cost given is an incremental cost added to the core fabrication cost; (2) no statement giving the out-of-core fuel inventory is made; (3) the fuel exposures are in metric tons; and (4) the final fissile plutonium content refers to the discharge mass.

3.7 Nuclear Data and Procedures

Cross Sections

In contrast to the previous four studies, which used libraries based on YOM cross sections[5], the AI preliminary work used the Mills cross section set[6], with more detailed analyses being based on a specific AI data tape. The specific cross sections used for the review calculations are from Ref. 11. As is indicated by AI Vol. III, a considerable amount of careful effort has been expended in the automating of data handling procedures. For this particular concept, the treatment of neutron spectra, and the averaging of cross sections over energy to obtain the group constants are likely to be of particular significance. This is illustrated throughout the report [e.g., the 15/35 group difference (AI, Page II-B-16), the sensitivity of the predicted sodium void worth to the associated change in spectrum (AI, Page III-B-12)].

The spectrum assumed for weighting of all except the graphite region is obtained from a fundamental mode calculation for the fast region composition only. While this spectrum may be adequate to obtain a reasonable estimate of the fast region neutron balance, the blanket spectrum is clearly and intentionally much different. Because a major feature of the AI design is the utilization of moderation to effect a change in Doppler effect and to alter the sodium void worth, careful attention to the blanket spectra should have been basic to the study. The facility for correctly treating

spatially varying neutron spectra in sufficient detail to allow calculation of group constants does not exist, and this lack of capability is of some concern for all concepts. Surveys of the effect of different spectral representations can, however, be used to define the range of uncertainty introduced by this problem. Such a study is not included in the AI report. Further, the use of Fe scattering cross sections in place of those for stainless steel (AI, Page VII-D-20) is probably adequate but does not seem consistent with the detail used in weighting. The AI study used a fission spectrum based on U^{235}, even though a spectrum which is presumably more appropriate is available (cf. Ref. 12, p. 23).

Geometric Representation

Several geometric representations were used in obtaining the results reported (AI, Page III-B-3). In general, these were well chosen. Certain of the approximations involved were checked by simple comparisons [S_4 versus diffusion theory (AI, Page VII-D-1)].

These calculations have been extended somewhat by LASL. The two specific representational approximations questioned were the axial 2-D effects within a given cell and the possible S_n effect on control rod worth. Table 3.6 summarizes the results of a set of 1- and 2-D problems, using diffusion theory (CRAM)[7] and an S_4 approximation (DDK, DTF)[8,9] for a single-reflected module. Comparable AI diffusion theory results are also shown in Table 3.6. It is clear that no significant differences are seen for any of these representations.

Table 3.6

LASL Comparison of Various Representations

	2D CRAM	DDK	1-D CRAM	DTF*	AI*
Reference k	1.0109	1.0157	1.0078	1.0224	1.000
Na Void Effect (%Δk)	-0.6	-0.36	-0.24	+0.04	-0.63
Central Control Rod Worth (%Δk)	4.6	4.4	4.7	4.8	4.4

* These figures are obtained using a 20 cm reflector savings with Na present, 25 cm with Na voided. The DTF case with a constant 20 cm reflector savings yields a -79%Δk Na void, rather than the +0.04%Δk.

The geometry and composition of the AI design had to be varied when ANL cross sections were used (see Appendix C). The k calculated by ANL varied from .935 to .948 depending on the method used to average the elastic removal cross sections. Table 3.7 gives the geometrical and compositional changes employed to bring the reactor critical.

Table 3.7

ANL Methods of Obtaining Criticality

Method of Averaging Graphite Elastic Removal Cross Sections	ELMOE		Average of ELMOE and 1/E		1/E	
k	——.935——		——.941——		——.948——	
Method of Obtaining Criticality	Core Fissile Content	Core Radius	Core Fissile Content	Core Radius	Core Fissile Content	Core Radius
Fissile Percentage at Criticality	26.8	23.2	26.5	23.2	26.2	23.2
Radius of Core at Criticality (cm)	28.5	33.3	28.5	33.0	28.5	32.6
Radius of Module at Criticality (cm)	56.6	61.4	56.6	61.1	56.6	60.7

4.0 FUEL AND MATERIALS

4.1 Fuel

Atomics International appears to support the conclusion in COO-279 that no clear-cut choice can be made at this time between the oxide and carbide fuel. Atomics International states that the oxide fuel appears to have the best near-term potential for economic operation of a fast reactor while the mixed carbide fuel with a sodium bond appears to have the best long-term potential for low fuel cycle costs.

The reference fuel of the AI study consists of 86% dense pellets having a composition of 60% UO_2 - 40% PuO_2 and an O/M ratio of 2.01. The thermal conductivity and melting point values selected by AI for this hyper-stoichiometric fuel appear to be high. Atomics International used a value of 0.033 watts/cm-°C for the thermal conductivity of the mixed oxide fuel; however, for UO_2 a value of 0.02 watts/cm-°C is generally used. The solution of plutonium oxide in the UO_2, the influence of irradiation (100,000 MWD/MT), and the excess oxygen should lower the thermal conductivity of the fuel. A more conservative value such as 0.01 watts/cm-°C would seem to be more appropriate. Atomics International has selected a value of 4900°F (2705°C) as the melting point of the mixed oxide fuel. This melting point value would represent the starting material; however, it will be reduced by fission product buildup. Insufficient data are available concerning the properties of the mixed oxide fuel. Therefore, many of the pertinent values of the mixed oxides are assumed to be similar to those of UO_2. The melting point of unirradiated UO_2 is about 5000°F (2870°C). The melting point of UO_2 is reduced to 4800°F (2550°C) after 45,000 MWD/T, and to 4450°F (2455°C) after 100,000 MWD/T. If these ratios are applied to the AI fuel which contains 40% PuO_2, approximately half of the fuel will be molten. If the lower thermal conductivity value is used, extensive melting of the fuel may take place.

The AI report is not clear as to the extent that the blanket fuel element stability was considered. The blanket region takes an added importance because of its high power density, extensive burnup, and nonvented fuel design. Based on the corrosion data presented on Page III-D-30, the clad thickness may be reduced to 5 mils at the end of the blanket life.

4.2 Other Materials

The value of 15,800 psi for the creep rupture strength of Type 304 SS in the AI report is based on a 1000-hour test. The temperature is not given. The fuel element is expected to last 16,200 hours (22½ months). The creep rupture strength values of Type 304 SS (ASTM 124 Rev.) for 10,000 hours are 15,000 psi at 1200°F and 9,000 psi at 1300°F. Extrapolation of the 10,000 hour values to 16,200 hours would reduce the creep strength values to 60%. These values should again be reduced by 25% to allow for irradiation damage.

THIS PAGE

WAS INTENTIONALLY

LEFT BLANK

The 15,000 cycles in fatigue as shown on Page III-D-31 for the thermal stresses calculated should be lowered because of slow fatigue cycles. Superimposed on these thermal stresses is the differential expansion strains from oxide-cladding interactions (Page III-D-33), and even a small cyclic strain of 0.5% would seriously limit the number of cycles.

The chemistry of the Type 304 SS was not specified in the AI report. It is important that the boron content as well as the amounts of ferrite- and austenite-forming elements be specified. The carbon content and grain size of the steel should also be specified.

The AI design shows no reflector around the reactor core. Consequently, the pressure vessel will be subjected to a considerable flux of neutrons over the 35-year life of this vessel. The chemistry of the Type 304 SS should be given considerable attention in order that severe embrittlement of the steel does not result. The locations of the welds on the inlet and outlet sodium nozzles are not known. The placement and type of thermal shields used in these areas are important.

The combination of carbon steel and stainless steel in the sodium system should be given further review since the stainless steel may become carburized by the combination at the operating temperatures.

A considerable development effort may be required before any assurance can be gained on the satisfactory performance of the B_4C control rods, under the expected reactor operating conditions. The compatibility of the B_4C and stainless steel will need to be determined.

APPENDIX A

INFERRED BREEDING RATIO CONTRIBUTIONS

Atomics International Table IV-B-3 contains sufficient data to obtain estimates of the effective breeding ratio contributions of the various regions. In Table A-1, certain relevant factors from AI Table IV-B-3 are repeated; the fissile contents reported are tanslated to kg. The fissile destruction by region is estimated, assuming 1.1 g fissile destruction per MWD. The lifetimes given then permit estimates of production and destruction of fissile material per year. This destruction rate is proportional to the power by region.

At this point, it is necessary to define an integral breeding ratio. The convenient definitions of integral breeding ratio (Ref. 10) are not strictly equivalent to the differential definition stated in the four reactor study ground rules. The breeding ratio here is calculated from

$$BR = \frac{\text{Net Fissile Produced + Fissile Destruction}}{\text{Fissile Destruction}} = \frac{\text{Total Fissile Produced}}{\text{Fissile Destruction}}$$

The destruction of fissile material is estimated from the power extracted as being 806 kg/year. The regionwise contributions shown in Table A-1 are net Pu produced in that region per total Pu destruction for the entire system.

Table A-1

Estimation of Breeding Ratio Used in AI Economic Evaluation

	Fast Region	(Axial)	Inner Blanket	(Axial)	Outer Blanket	(Axial)	Exterior	(Axial)	Peripheral
Exposure* (MWD/kg	99	5.5	48.1	5.0	37.4	4.2	59.4	6.2	2.4
Power (Mw)*	1388	55	538	40	200	16	187	14	12
Loading (kg U + Pu)*	8010	5720	12750	9100	6090	4350	7790	5560	12400
Initial Fissile* a/o	27.3	--	--	--	--	--	--	--	--
Final Fissile* (a/o)	22.63	2.99	6.25	2.65	5.85	2.41	5.68	2.16	1.96
Initial Fissile (kg)	2187	--	--	--	--	--	--	--	--
Final Fissile (kg)	1600	171	756	341	356	105	442	120	243
Lifetime (yr)*	1.96	1.96	3.91	3.91	3.91	3.91	8.46	8.46	8.46
Net Prod/yr kg	-300	87	193	61	91	26	52	14	28
Breeding Gain (Partial; Fissile Destruction = 806 kg/yr)	-.37	0.11	.24	0.08	0.11	0.03	0.06	0.02	0.03

TOTAL BREEDING RATIO = 1.31

*As given in AI Table IV-B-3

APPENDIX B

MODEL USED FOR LASL REVIEW CALCULATIONS

Figure B-1 is a schematic representation of the model, including zone numbers. Table B-1 presents the various material mixtures used, while Table B-2 identifies each region with its mixture in the given classes of calculations. Note from Table B-2 that for the reference case (i.e., control rod up and Na in), regions 1-6 have mixtures identical to those given for these regions in AI, Table III-B-2, and that in the 2-D reference case, region 7 is identical to region 1. Also, the mixtures of regions 9, 10, and 11 are the same as for regions 3, 4, and 6, respectively, with the following exceptions: Total heavy atoms (including fission product pairs) are kept the same in the above corresponding regions, while the 275 kg of Pu-239 in the axial blankets* is divided between regions 9, 10, 11 in proportion to the top leakages calculated by AI;[11] 1/0.564/0.286. The ratio of fission product pairs to Pu-239 for these regions is the same as this ratio for the radial blankets (regions 4 and 6). The remaining U-238 in each axial blanket region was then determined so as to conserve heavy atoms.

The results of the various k calculations are summarized in Table B-3, along with the resultant Na void and rod worths. As may be seen in the table, both 1-D and 2-D calculations were performed in diffusion theory using CRAM and S_n transport approximation, using the S_4 options of DTF and DDK. Fractional fission neutron yields (Ref. 12, page 20) in each group (χ's) for U-235 were used in these calculations in order to be consistent with the AI calculations, although they may not be the most appropriate available data for Pu-fueled reactors. The AI cross section set was used for the review calculations.

Some of the DTF calculations in Table B-3 were, for comparison purposes, repeated, using the Hansen-Roach cross section set[12] and Pu-239 χ's (Ref. 12, Page 23). Also, for comparison purposes, an S_8 calculation was performed for the reflected reference case. The results are shown in Table B-4. It is apparent that little is gained by going from the S_4 to S_8 approximation. The control rod worth was quite insensitive to the cross section set and χ's used, although the Na void worths show some change.

One significant difference is present in the review calculations performed. In the previous review, an attempt was made to describe the entire system in two-dimensional calculations. The AI design, however, has two significant features which made this more difficult. The first is the strong and important variation in spectrum between regions; the second is the strong coupling among modules. Each of these features tends to make the approximate procedures used in the previous review less applicable for the AI concept. The attempt in this review has been directed more toward evaluating specific effects, placing more reliance on certain AI calculations. It is thus even more basic here than in the previous review to consider relative rather than absolute results in formulating conclusions.

---

*Note that this value (Ref. 11) supersedes the value 163 kg Pu given on AI, Page III-B-6.

[for 1-D model, buckling height = 171 cm for Na in
= 181 cm for Na out]

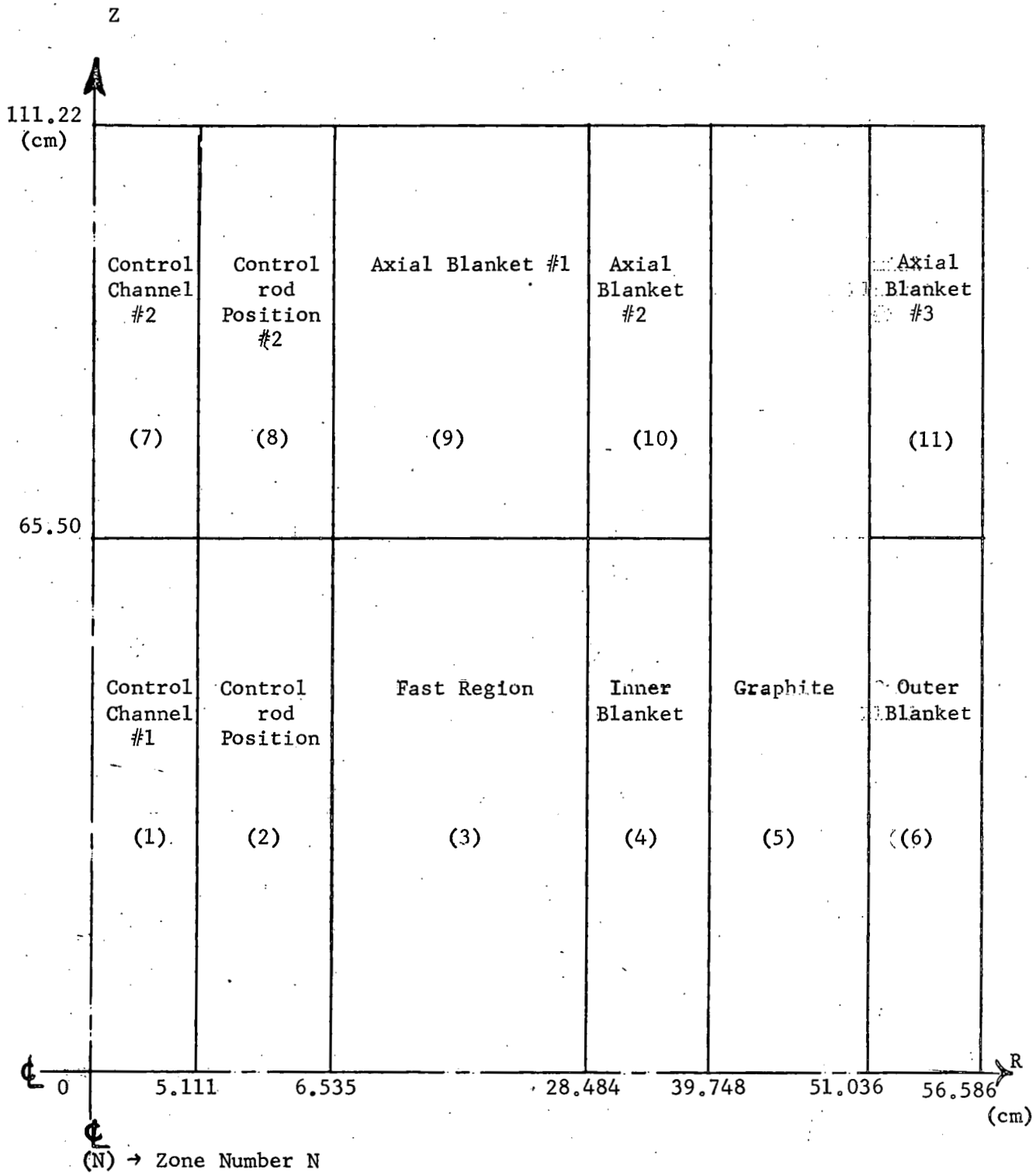

Figure B-1 ATOMICS INTERNATIONAL 1000 MWe FAST REACTOR CALCULATIONAL MODEL

Table B-1

AI 1000 MWe Fast Reactor Calculational Model

Mixture Number Densities

Material	Mixture A	B	C	D	E	F	G	H	I
304 SS	2.066 -2	1.2786 -2	1.0338 -2			1.2786 -2	1.0338 -2	1.0338 -2	
Na	4.206 -3	1.17015-2	8.202 -3			1.17015-2	8.202 -3	8.202 -3	
0		1.3166 -2	2.12348-2			1.3166 -2	2.12348-2	2.12348-2	
U^{238}		4.0433 -3	1.0084 -2			6.3358 -3	1.04775-2	1.05259-2	
Pu^{239}		1.3349 -3	3.658 -4**			1.696 -4	9.56 -5	6.24 -5	
Pu^{240}		6.697 -4							
Pu^{241}		9.91 -5							
Pu^{242}		2.44 -5							
f.p. pairs		4.114 -4	1.67 -4			7.74 -5	4.37 -5	2.85 -5	
C				8.374 -2	1.36155 -2				2.7231 -2
B^{10}					1.02385 -2				2.0477 -2

	B1 (reflected)*	B2 (free)*
U-238	4.1752 -3	3.6533 -3
Pu-239	1.265 -3	1.540 -3
Pu-240	6.349 -4	7.726 -4
Pu-241	9.40 -5	1.14 -4
Pu-242	2.31 -5	2.82 -5
f.p. pairs	3.900 -4	4.746 -4

*Mixtures B1 and B2 are the DTF calculated new heavy atom number densities determined by a concentration search on Pu-239, -240, -241, -242, and f.p. pairs holding total heavy atoms (including f.p. pairs) constant.

** The figure given in Table III-B-2 for the inner blanket appears to be in error.

Table B-2

Region Mixtures for Various Calculations

Region	Control Rod Up		Control Rod Down	
	1-D	2-D	1-D	2-D
1[(a)]	A	A	A	A
2[(a)]	A	A	I	I
3[(a)]	B	B	B	B
4	C	C	C	C
5	D	D	D	D
6	C	C	C	C
7	-	A	-	A
8	-	E[(b)]	-	A
9	-	F	-	F
10	-	G	-	G
11	-	H	-	H

(a) In the calculations with Na out of regions 1, 2, and 3, the control rod is up and there is, of course, zero Na number density in these regions.

(b) Half-densities were used for the withdrawn control rod to account for reflected region symmetry (with respect to Z = 0).

Table B-3

k; Rod and Na Void Worths

[Using AI Cross Sections, U-235 χ's]

Conditions (a)	Outer B.C. (b)	k 1-D Results CRAM	1-D Results DTF	1-D Results CRAM	1-D Results DDK
Reference Case	R	1.0078	1.0224	1.0109	1.0157
	F	0.9075	0.9293		
Na out of Regions 1, 2, & 3	R	1.0054	1.0228	1.0049	1.0121
	F	0.8910	0.9173		
Control Rod Down	R	0.9610	0.9747	0.9648	0.9713
Graphite Replaced by Radial Blanket	R		1.0070		
	F		0.9191		
Graphite Replaced by Radial Blanket, Na out of Regions 1, 2, & 3	R		1.0062		
	F		0.9056		
Na Void Worth (Δk)	F	-0.0165	-0.012		
	R	-0.0024	+0.0004	-0.006	-0.0036
Control Rod Worth (Δk)	R	0.0468	0.0477	0.0461	0.0444

(a) Unless explicitly stated otherwise, Na is assumed in entire module and control rod is assumed to be up.

(b) R = reflected; i.e., $d\phi/dx = 0$

F = free; i.e., $\phi = 0$ at extrapolated boundary in diffusion theory (CRAM); and vacuum condition (no return flux) in S_n transport approximation (DTF and DDK).

Throughout this review, "fast region" is used to refer to region (3) indicated on Fig. B-1. The term "core" is used to include the fast region and central control regions Regions [(1), (2), and (3) of Fig. B-1] . "Blanket" is used to refer to any or all of the blanket regions indicated in Fig. B-1 [Regions (4), (6), (9), (10), and (11)] plus the graphite (5). "Coupling" is used to refer to module-to-module coupling only.

Table B-4

k; Rod and Na Void Worths Calculated by DTF,
Using Hansen-Roach Cross Sections and Pu^{239} χ's

Condition	Outer B.C.	S_n	k
Reference Case	Reflected	4	0.9842
	Reflected	8	0.9830
	Free	4	0.8895
Na out of regions 1, 2, & 3	Reflected	4	0.9889
	Free	4	0.8825
Control Rod Down	Reflected	4	0.9367
Na Void Worth (Δk)	Reflected	4	+0.0047
	Free	4	-0.0070
Control Rod Worth (Δk)	Reflected	4	0.0475

APPENDIX C

MODEL USED FOR ANL REVIEW CALCULATIONS

The geometry and compositions used for the ANL review calculations were taken from AI Table III-B-2. To achieve criticality, two methods were used:

(1) The core region radius was increased by 4.5 cm.

(2) The enrichment of the fast region was increased from 23.2% to 26.5% of fissionable to total heavy atoms.

Radial 1-D calculations were performed using a reflected boundry condition ($d\emptyset/dr = 0$). An axial reflector savings of 20 cm was used in the regions with sodium and 22.5 cm was used in the regions of 50% sodium void.

Fission and capture cross sections were generated by the Argonne cross section code MC^2. This code calculates cross section for 0.25 lethargy groups, which were then collapsed to the 26 groups used in the calculations. Fission and capture cross sections above 25 kev were assumed independent of temperature and composition. Below 25 kev resonance integral calculations were performed. Goldstein-Cohen interpolation was used between narrow and wide resonance calculations and heterogeneity was taken into account by equivalence theory. Flux correction factors were used to provide an approximate fertile-fissile overlap correction.

Light element scattering cross sections were generated with the ELMOE code. Transport and elastic removal cross sections for voiding sodium were obtained by subtracting the appropriate macroscopic cross sections for the voided case from those for the unvoided case and divided by the atom/cc of sodium voided.

Blanket homogenized macroscopic cross sections were obtained by running ELMOE with $B^2 = 0$ and inputting the fission spectrum source of the fast region.

Three different carbon elastic scattering cross sections were used:

(1) The scattering cross section averaged over the ELMOE spectrum.

(2) The scattering cross section averaged over a 1/E spectrum.

(3) An arithmetic average of the two cases above.

APPENDIX D

SODIUM VOID CORRECTIONS - FOUR ORIGINAL 1000 MWe DESIGN STUDIES

It is now believed that the ANL calculations used to modify the LASL calculations in COO-279 gave too negative a sodium void effect because of the use of values of the Pu^{239} fission cross section that were too large at low energies, particularly between 1 and 4 kev. The values used are indicated in Table D-1. Also given are the ANL cross sections[14] used in the comparison calculations[13] presented at the October 1965 Fast Breeder Conference at Argonne, the cross sections used by AI, and Los Alamos cross sections from the Petrel bomb test.[15] The last numbers are very rough as they represent a sight average of data with considerable fluctuations, but they do indicate that the values used in the original ANL calculations in this range are undoubtedly too high. While this discrepancy should not significantly affect other quantities, it leads to too negative a sodium void effect because it increases low energy neutron importance and thereby reduces the energy variation of the importance function. On the other hand, it is quite possible that the ANL cross sections are too low below about 500 ev, which produces the opposite effect. This is probably less important, however, than the effect mentioned previously. This is balanced by the fact that the ANL October 1965, Pu^{239} fission cross sections in Table D-1 were prepared not taking account of the data of P. White,[16] according to which the cross section in the energy range 20-100 kev is considerably lower than shown in Table D-1. The use of the White data would cause the sodium void effect to be more positive by the order of 0.5% k for complete expulsion of sodium from the reactor core, while a reasonable estimate of how much more negative the void effect could be as a result of higher fission cross sections in the energy region below 500 ev is about -0.5% k.

It has been stated repeatedly that there is considerable uncertainty in sodium void effect calculations because of cross section uncertainties. It has been found that uncertainty in the Pu^{239} fission cross section is particularly serious.[14] However, it is believed at ANL at the present time that the sodium void effect should have been calculated to be more positive than was indicated by the ANL calculations in COO-279. Adjustments to the sodium void effect for complete voiding of the core based on comparison of calculations using the original ANL cross sections and those of October 1965, are given in Table D-2.

Because the ANL calculations were previously found to be in reasonable agreement with those of three of the contractors before, evidently they are now in disagreement. In the case of GE, this is probably consistent with the disagreement found in the October 1965 comparison calculations.[13,14] In the comparison calculations, the ANL results were much more positive than those obtained by AI with the same cross sections used in the present study.[13,14] This disagreement is reflected to some extent in the results of the evaluation calculations, but the discrepancies are relatively small in the present case

because of the low ratio of fertile to fissile material employed by AI in the core regions.

The adjustment indicated in Table D-2 now brings the modified value of sodium void effect for the CE to 2.9% k, in reasonable agreement with the 2.4% k calculated by CE. In the other cases, the modified sodium void effect now becomes considerably more positive than calculated by the contractors. The whole process of arriving at these numbers was so indirect and approximate, however, that the exact values quoted should not be taken seriously, particularly for the purpose of assessing the merits of one design relative to those of another. There is strong indication, however, that the criterion, for example, of essentially zero reactivity gain from uniform sodium voiding from the core might be hard to meet with any of the designs. This again points to the importance of better determining what the criteria should actually be.

Table D-1

Comparison of Pu^{239} Fission Cross Sections[a]

Group	E_L, kev	σ_f of Pu^{239}, Barns			
		Used in ANL Calc. in COO ($T=300^oK$, $\sigma_p=300$)	ANL October, 1965 ($T=1500^oK$, $\sigma_p=400$)	AI	Estimated from Petrel[15]
1	[illegible]	1.90	1.9	1.94	
1	3.68 Mev	1.90	1.90	1.94	
2	2.27	1.95	1.95	1.96	
3	1.35	1.97	1.97	1.98	
4	0.820	1.82	1.82	1.87	
5	0.498	1.64	1.64	1.68	
6	0.302	1.57	1.57	1.66	
7	0.183	1.56	1.56	1.66	
8	0.110	1.60	1.60	1.66	
9	0.0674	1.73	1.73	1.93	
10	0.0409	1.94	1.89	2.02	
11	0.0248	2.14	1.90	2.02	
12	15.0 kev	2.30	1.90	2.10	
13	9.12	2.43	1.88	2.36	
14	4.31	2.89	2.38	2.36	2.3
15	2.61	3.35	3.04	4.00	2.0
16	2.03	4.63	3.75	5.7	2.0
17	1.23	6.54	4.50	5.7	3.0
18	0.961	6.54	5.39	5.7	
19	0.583	6.80	6.36	5.7	
20	0.275	10.5	8.41	11.3	
21	0.101	12.0	12.1	14.1	
22	0.029	12.7	13.2	13.5	

(a) There is some inconsistency in the values of temperature and σ_p, the reactor scattering cross section per reacting atom, at which the fission cross sections tabulated here were evaluated. This is not important for the present discussion, however.

Table D-2

Adjustments to ANL Calculations for Complete Voiding of Sodium from Core, $\%\Delta k$

	Adjustment	Modified 2-D Value*
AC	1.2	1.2
CE	1.9	2.9
GE	1.8	2.2
W	1.3	1.6

*Base 2-D calculation of COO-279, modified with 1-D calculations with ANL cross sections.

APPENDIX E

NORMALIZED FUEL CYCLE COSTS

The fuel cycle costs, as presented in the A-C, W, GE, and CE Design Studies, were given in COO-279. The fuel cycle costs for the five studies have been recalculated using a consistent set of ground rules and adjusting certain cost components to account for differences between the fuel element designs and the fuel management programs of the Design Studies. The result of the recalculation is as follows:

	A-C	W	GE	CE	AI
Fabrication	.504	.458	.816	.626	.423
Reprocessing	.271	.240	.276	.264	.252
Pu Inventory	.603	.633	.427	.249	.426
Shipping	.052	.040	.054	.044	.036
Fabrication Charge	.081	.092	.090	.058	.060
Pu Credit	(.320)	(.549)	(.219)	(.387)	(.280)
Total	1.191	.914	1.444	.854	.917

Fuel cycle cost data applied to all design studies were as follows:

Core burnup, ave.	100 MWD/kg(U + Pu)
Plant factor	80%
Fissile Pu value	$10/gram
Interest on core Pu	10%/year
Reprocessing plant Pu criticality limit	67% of U^{235} limit
Reprocessing plant charge	$23,000/day
Shipping cost, core & axial blanket	$20/kg
Shipping cost, radial blanket	$10/kg
Fabrication cost	Adjusted for design
Fuel fabrication charge	10% of book value
Uranium conversion	$5.60/kg
Fabrication losses	1%
Reprocessing losses	1% included in the Pu credit

A cost of $300/kg for core and axial blanket oxide fuel fabrication ($350/kg for carbide) and $70/kg for radial blanket fabrication was used as a base for determining fabrication cost for the individual design studies. These costs were adjusted for variation in pellet diameter by assuming it would cost

$60/kg to press core and axial blanket oxide pellets of 0.25-inch diameter ($68/kg for carbide) and $14/kg to press radial blanket pins of 0.340-inch diameter. Figure V-4 of the AI Feasibility Study was used to derive the pellet pressing charge for other size pellets.

The cost of encapsulation was assumed to be $75/kg for an oxide core and axial blanket having 2.2 pins/kg and $17.5/kg for radial blanket pins having 1.0 pin/kg. A proportional relationship between the encapsulation charge and pins/kg value was assumed. The remainder of the fabrication cost was considered to be independent of fuel assembly design.

The reprocessing costs assumed mixing of all discharged fuel. The reprocessing rate (67% of the U^{235} rate) was calculated using the total Pu enrichment rather than fissile Pu enrichment. The reprocessing time was based on the hypothetical AEC reprocessing plant described in TID-7025.

The out-of-core inventory was calculated on the basis of 350 days for cooling, all shipping, reprocessing, fabrication, and new fuel storage. In addition, each reactor was assumed to be part of a large system of fast reactors such that the fuel loses its identity with the reactor once it is delivered to the reprocessing facility. While this is far from the situation that will exist with the first plants, it was used for this study because it prevents excessive penalization of those plants whose fuel management programs do not fit well with the rather arbitrarily selected out-of-core days. (Thus, a plant with a cycle life of 180 days and 1/3 of the core removed at each refueling has an out-of-core inventory of approximately 2/3 the in-core value rather than an out-of-core inventory equal to the in-core inventory, which would be an excessive penalty for exceeding the 350-day out-of-core time by 10 days.)

The large increase in the fabrication cost for the GE study is a reflection of the normalization of the fabrication cost for pin diameter and length and also the assumption of equal core and axial blanket fuel fabrication cost. The significant increase in the CE fabrication cost is the result of an increase from $124/kg for core and axial blanket fuel fabrication to $314/kg.

The increase in the reprocessing costs for all studies is largely a result of the $23,000/day charge for the reprocessing plant; also the Pu criticality limit was based upon the total Pu enrichment rather than the smaller fraction of fissile Pu isotopes.

The assumption of private ownership of nuclear fuel resulted in an increase in the Pu inventory charge for all studies, and in addition, for GE and AI the out-of-core inventory was increased over that assumed in the respective Design Studies.

Table E-1

Data for Fuel Cycle Cost Calculation

	A-C	CE	GE	W	AI
Fuel Cycle Life, Days	349	74.5	168	228	238
Fraction of Core Replaced/Refueling	.333	.125	.222	.167	.333
Fraction of Radial Bl. Replaced/Refueling	.250	.0417	.125	.123	.1667/.0769
Core Plus Axial Bl. Discharge/Refueling,kg	6656	2594	7108	5261	4576
Radial Blanket Discharge/ Refueling,kg	21692	1163	3076	7019	7363
Energy/Cycle, kwhr x 10^{-9}	6.69	1.43	3.22	4.37	4.56
Core & Axial Blanket Fabrication, $/kg	331	314	341	298	304
Radial Blanket Fabrication $/kg	54	69	66	61	72
Fissile Pu, kg/yr	224	271	153	384	196
Ratio, out-of-core to in-core Fuel	.334	.587	.463	.256	.490

APPENDIX F

ERRATA TO COO-279, "AN EVALUATION OF FOUR DESIGN STUDIES OF A 1000 MWe CERAMIC FUELED FAST BREEDER REACTOR"

Page 1-9	The first sentence under C., Doubling Time, should read: "The doubling times, in years, as quoted in the Design Studies are: A-C, 19.5; CE, 6.2: GE, 15.8; W, 11.7. The doubling times were based on ground rules assumed by the contractors and are therefore not comparable. Doubling times based on Design Study data, but using a consistent calculational technique are given in Table 3.6. Doubling times, calculated using consistent physics data (also Table 3.6), are A-C, 30; CE, 7.2; GE, 20; and W, 19."
Table 2.1	The total pins in the W radial blanket region (page 3 of Table 2.1) should be 32,487, not 19,812.
Page 4-5	The seventh and eighth sentences under Oxide - Carbide Comparison should read: "Present irradiation data on the limits of carbide fuel and on the effect of carbon and uranium-plutonium diffusion are inconclusive. Diffusion of uranium-plutonium may be the important..."

REFERENCES

1. "Large Fast Reactor Design Study," ACNP-64503, Allis-Chalmers, Atomic Power Development Associates, Babcock and Wilcox Company, January 1964.

   "Liquid Metal Fast Breeder Reactor Design Study," CEND-200, Combustion Engineering, January 1964.

   "Liquid Metal Fast Breeder Reactor Design Study," GEAP-4418, General Electric Company, January 1964.

   "Liquid Metal Fast Breeder Reactor Design Study," WCAP-3251-1, Westinghouse, January 1964.

2. "An Evaluation of Four Design Studies of a 1000 MWe Ceramic Fueled Fast Breeder Reactor," COO-279, Reactor Engineering Division, Chicago Operations Office, U. S. Atomic Energy Commission, December 1, 1964.

3. "Feasibility Study of a 1000-MWe Sodium-Cooled Fast Reactor," NAA-SR-11378, Vols. I, II, and III.

4. AVERY, R., et al, "Theory of Coupled Reactors," P/1858, pp. 182-191, Geneva 1958.

5. YIFTAH, S., "Fast Reactor Cross Sections," Pergamon Press, 1960

6. MILLS, C. B., "Neutron Cross Sections for Fast & Intermediate Nuclear Reactors," LAMS-2255, January 1959.

7. HASSITT, A., "A Computer Program to Solve the Multigroup Diffusion Equations," UKAEA, TRG Report 229(R), 1962.

8. WORLTON, J. and CARLSON, B., "The DDK Code," an unpublished Los Alamos Scientific Laboratory Code.

9. CARLSON, et al, "DTF Users Manual," UNC Phys/Math-3321, November 1963.

10. SPINRAD, B. I., "On the Definition of Breeding," in "Proceedings of the Conference on the Physics of Breeding," ANL-6122, October 1959.

11. Private Communication from R. Sevy, Atomics International, September 29, 1965.

REFERENCES (continued)

12. HANSEN, G. E. and ROACH, W. H., "Six and Sixteen Group Cross Sections for Fast and Intermediate Critical Assemblies," LAMS-2543, December 1961.

13. OKRENT, D., "Intercomparison of Calculations," Proceedings of Conference on Safety, Fuels, and Core Design in Large Fast Reactors, Argonne National Laboratory, October 11-14, 1965, USAEC Report ANL-7120.

14. HUMMEL, H. H., "Sensitivity of Fast Reactor Parameters to Cross Section Uncertainties," Presented at the Conference on Neutron Cross Section Technology, Washington, D. C., March 22-24, 1966.

15. SHUNK, E. R., BROWN, W. K., and LA BAUVE, R., "Fission Cross Section of Pu-239, 20 eV to 2 MeV," Presented at the Conference on Neutron Cross Section Technology, Washington, D. C., March 22-24, 1966.

16. WHITE, P. H., HODGKINSON, J. G., and WALL, G. J., "Measurement of Fission Cross Sections for Neutrons of Energies in the Range 40-500 keV," SM 60/14 IAEA Symposium on the Physics and Chemistry of Fission, Salzburg, Austria, March 22-26, 1965.